

RESEARCH

Open Access



# Metabolic stress constrains microbial L-cysteine production in *Escherichia coli* by accelerating transposition through mobile genetic elements

Kevin Heieck, Nathanael David Arnold and Thomas Bartholomäus Brück\*

## Abstract

**Background** L-cysteine is an essential chemical building block in the pharmaceutical-, cosmetic-, food and agricultural sector. Conventionally, L-cysteine production relies on the conversion of keratinous biomass mediated by hydrochloric acid. Today, fermentative production based on recombinant *E. coli*, where L-cysteine production is streamlined and facilitated by synthetic plasmid constructs, is an alternative process at industrial scale. However, metabolic stress and the resulting production escape mechanisms in evolving populations are severely limiting factors during industrial biomanufacturing. We emulate high generation numbers typically reached in industrial fermentation processes with *Escherichia coli* harbouring L-cysteine production plasmid constructs. So far no genotypic and phenotypic alterations in early and late L-cysteine producing *E. coli* populations have been studied.

**Results** In a comparative experimental design, the *E. coli* K12 production strain W3110 and the reduced genome strain MDS42, almost free of insertion sequences, were used as hosts. Data indicates that W3110 populations acquire growth fitness at the expense of L-cysteine productivity within 60 generations, while production in MDS42 populations remains stable. For the first time, the negative impact of predominantly insertion sequence family 3 and 5 transposases on L-cysteine production is reported, by combining differential transcriptome analysis with NGS based deep plasmid sequencing. Furthermore, metabolic clustering of differentially expressed genes supports the hypothesis, that metabolic stress induces rapid propagation of plasmid rearrangements, leading to reduced L-cysteine yields in evolving populations over industrial fermentation time scales.

**Conclusion** The results of this study implicate how selective deletion of insertion sequence families could be a new route for improving industrial L-cysteine or even general amino acid production using recombinant *E. coli* hosts. Instead of using minimal genome strains, a selective deletion of certain IS families could offer the benefits of adaptive laboratory evolution (ALE) while maintaining enhanced L-cysteine production stability.

**Keywords** L-cysteine, *E. coli*, Minimal genome strain, Metabolic stress, Insertion sequences, Transcriptomics, Deep sequencing, Metabolic engineering

## Background

The amino acid L-cysteine, harbouring a thiol group, provides a high redox activity in cell metabolism, plays a crucial role in protein folding, functions as a catalytic residue of several enzymes and serves as a building block of 5-L-glutamyl-L-cysteinylglycine (GSH) and as a donor

\*Correspondence:

Thomas Bartholomäus Brück  
brueck@tum.de  
Technische Universität München, Lichtenbergstraße 4, 85748 Garching,  
Germany



© The Author(s) 2023. **Open Access** This article is licensed under a Creative Commons Attribution 4.0 International License, which permits use, sharing, adaptation, distribution and reproduction in any medium or format, as long as you give appropriate credit to the original author(s) and the source, provide a link to the Creative Commons licence, and indicate if changes were made. The images or other third party material in this article are included in the article's Creative Commons licence, unless indicated otherwise in a credit line to the material. If material is not included in the article's Creative Commons licence and your intended use is not permitted by statutory regulation or exceeds the permitted use, you will need to obtain permission directly from the copyright holder. To view a copy of this licence, visit <http://creativecommons.org/licenses/by/4.0/>. The Creative Commons Public Domain Dedication waiver (<http://creativecommons.org/publicdomain/zero/1.0/>) applies to the data made available in this article, unless otherwise stated in a credit line to the data.

compound of sulphur, which is required for the synthesis of Fe/S clusters, biotin, coenzyme A and thiamine [1, 2].

Besides the essential function in metabolism, L-cysteine is also of considerable industrial importance, with applications ranging from pharmaceutical products and cosmetics over food production to feed additives in livestock farming [3, 4].

To date, the cheapest and thereby most prevalent means of L-cysteine production involves chemical hydrolysis of—and extraction from—keratinous biomass, such as feathers, pig bristles and animal hair by means of electrolysis [5]. Up to 27 tons of hydrochloric acid are required to obtain 100 kg of a racemic mixture of cysteine from 1.000 kg raw material [5, 6]. In order to circumvent negative impacts upon the environment associated with hydrochloric waste disposal, alternative technologies such as fermentation and enzymatic conversion have been explored and rapidly gained significance since their implementation. In 2004, 12% of the globally manufactured L-cysteine global originated from fermentation [7].

The enzymatic conversion of DL-2-amino- $\Delta^2$ -thiazoline-4-carboxylic acid (D-ATC) to L-cysteine with *Pseudomonas* spp. derived enzymes is limited by product inhibition [8, 9]. For biotechnological L-cysteine production, the bacteria *C. glutamicum* and *E. coli* harbouring optimised plasmids represent the dominant expression organisms. Since titres from *C. glutamicum* are low (approx. 950 mg/L), *E. coli* is the preferred host for L-cysteine production by fermentation [10].

However, there are still major obstacles in upscaling fermentation processes with engineered microorganisms. The stability of strains with synthetic production is highly fragile and presents a challenge when implementing bioprocesses on a large scale [11, 12]. The introduction of designed plasmid constructs and the upregulation of the genetic elements for recombinant L-cysteine production pose a defiance to the tightly regulated homeostasis within host cells [13, 14]. This metabolic load hinders the expression of other genes, thereby negatively affecting growth rate and promoting evolutionary pressure [15–17]. Furthermore, L-cysteine has an inhibitory to toxic effect on *E. coli* cell growth, depending on the concentration present in cells [18]. In microorganisms, several concepts are reported that can lead to a selection advantage and thus to both phenotypic and genotypic variation within populations [19, 20]. In bacteria, activation of mobile genetic elements, such as insertion sequences (IS) and corresponding transposons can lead to mutagenesis-based inactivation of synthetic constructs [21]. In addition, expression of regulatory elements of the SOS response has been shown to increase the expression of error-prone DNA polymerases, which can indirectly induce further mutations in recombinant gene elements,

such as plasmids [22, 23]. These effects have a negative impact on the time dependent-productivity (space–time yield) and consequently the total yield of the biomolecule to be produced. This observation is especially relevant in continuous fermentations, where populations reach high generation numbers while being exposed to prolonged metabolic stress [24, 25].

Metabolic engineering of *E. coli* strains optimising L-cysteine production, targets the overexpression of specific bottleneck genes (Fig. 1). In order to capture 3-P-glycerate from glycolysis and feed it into the synthesis of the precursor amino acid L-serine to finally convert it to L-cysteine, the two feedback-resistant genes *serA* and *cysE* are overexpressed [26, 27]. An L-cysteine production pathway uncoupled from glycolysis involves the assimilatory reduction of sulphate. With the expression of *cysM*, assimilated thiosulphate is converted to L-cysteine via an intermediate step. Since large amounts of L-cysteine have an inhibitory growth effect on *E. coli* cells, the overexpression of an L-cysteine efflux gene (*eamA*) is essential [28].

The aim of this study was to investigate the genotypic and phenotypic alterations of engineered L-cysteine producing K-12 MG1655 derived *E. coli* strains leading to L-cysteine production decline. For the first time, a combined omics-approach was applied in order to unravel the underlying mechanisms within an industrially relevant L-cysteine production system. Therefore, the *E. coli* production strain W3110 and a reduced genome strain (MDS42) free of transposable elements were selected. By simulating long-term cultivations in shaking flasks, we achieve generation numbers (>60) of industrial fermentation processes. In accordance with our hypothesis, a L-cysteine productivity collapse of up to 85% could be detected on a laboratory scale. Using differential transcriptomics, we uncover strong shifts in L-cysteine and sulphur stress related transcripts between early and late populations. Furthermore, Illumina-based plasmid deep sequencing data strongly suggested that predominantly IS3 and 5 family transposases induce rapid plasmid rearrangements. Both observations, presumably in combination, disrupt L-cysteine production in late W3110 populations while L-cysteine production in MDS42 populations remain stable, further supporting the involvement of insertion sequences.

## Results and discussion

### Stability of L-cysteine-producing phenotypes

To study phenotypic and genetic diversities in L-cysteine producing *E. coli* populations over timescales relevant on industrial levels, we simulated a gradual scale-up growth process (Fig. 2).

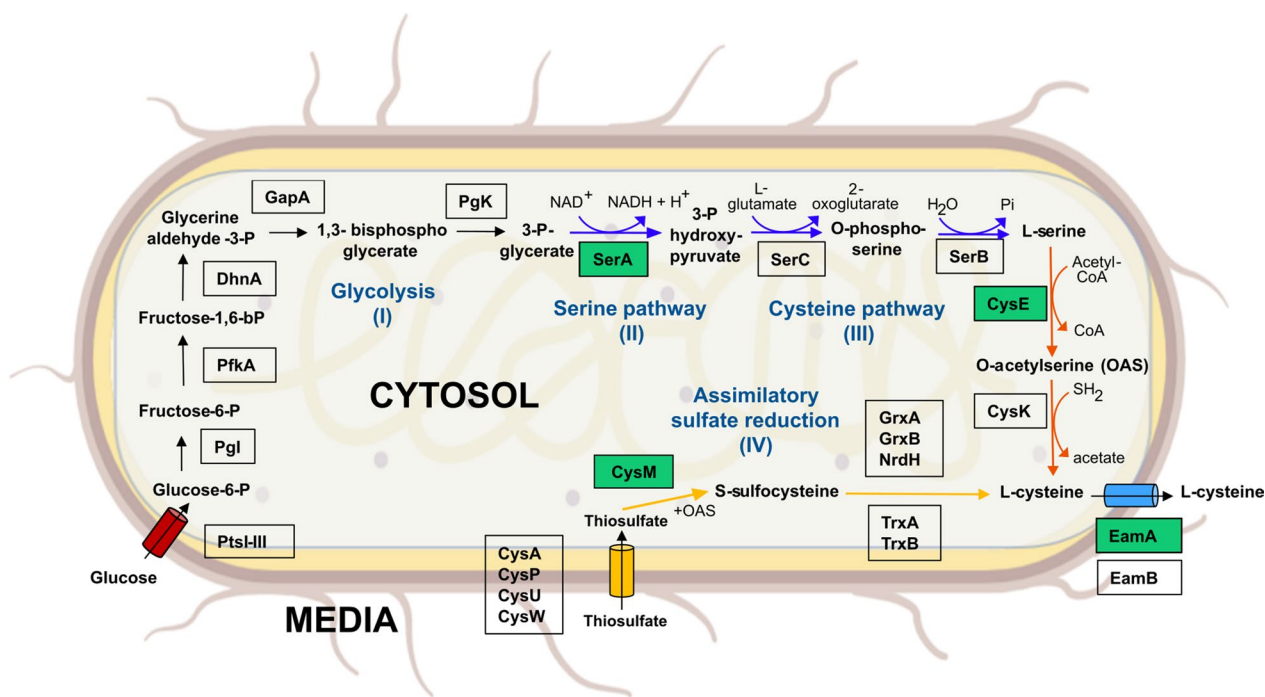


**Fig. 1** Metabolic engineering strategies for L-cysteine biosynthesis in *Escherichia coli*: Through glycolysis (I, black arrows), the essential intermediate 3-phospho-glycerate is produced, which is incorporated into L-serine biosynthesis (II, blue arrows). As a precursor amino acid, L-serine is used for the formation of L-cysteine (III, orange arrows). Alternatively, L-cysteine can be synthesised by the assimilatory sulphate reduction pathway (IV, yellow arrows). L-cysteine is transported out of the cell. Corresponding proteins for conversion of substrates are shown in black boxes. Boxes with green background represent expressed proteins within the synthetic plasmid constructs in this work. *PtsI-III* Phosphotransferase system I-III, *Pgl* Glucose-6-phosphate isomerase, *PfkA* Phosphofruktokinase 1, *DhnA* Fructose-bisphosphate aldolase, *GapA* Glyceraldehyde-3-phosphate dehydrogenase A, *PgK* Phosphoglycerate kinase, *SerA* D-3-phosphoglycerate dehydrogenase, *SerC* Phosphoserine aminotransferase, *SerB* Phosphoserine phosphatase, *CysE* Serine acetyltransferase, *CysK* Cysteine synthase A, *CysA,P,U,W* ATP-dependent sulphate/thiosulphate uptake system, *CysM* Cysteine synthase B, *GrxA,B* Glutaredoxin 1,2, *NrdH* Glutaredoxin-like protein, *TrxA,B* Thioredoxin 1,2, *EamA,B* Cysteine exporter. Created with BioRender.com

We cultivated the minimal genome strain MDS42, almost free of any insertion sequences (IS), next to the traditional K-12 strain W3110 to determine potential effects of transposable elements that disrupt synthetic constructs. Specifically, we cultivated three different clones of two *E. coli* strains, each with an L-cysteine producing plasmid (Fig. 3A). The original plasmid pCYS possessed bottleneck genes for L-cysteine biosynthesis with the corresponding genomic promoter regions (Fig. 3A). *CysE* and *SerA* are feedback insensitive variants as described in references [26, 27, 29, 30]. For cloning of pCYS\_i the genes were arranged in one operon with GAPDH as a constitutive promoter. Furthermore, non-coding backbone sequences were trimmed to potentially alleviate metabolic burden on production cells. The plasmid pCYS\_m carries the additional gene *cysM*, coding for cysteine synthase B, under the control of the stationary phase promoter *pfic*. This way, L-cysteine production should be shifted to the stationary phase, therefore temporally uncoupling cell growth from L-cysteine biosynthesis during the 72 h re-cultivations.

In order to prevent plasmid loss, we kept the cultures at a constant antibiotic selection. By serially transferring the W3110 production strains every 10 h and the MDS42 production strains every 5 h (due to its higher growth rate), we achieved populations >60 cell generations (Additional file 1: Table S2). Hence, an exponential growth phase was guaranteed at all times throughout the experiment. At each transfer step, we sampled the growing *E. coli* populations and immediately cryopreserved them, in order to study time dependent phenotypic and genetic variability following a 72 h re-cultivation of the respective culture samples.

Final L-cysteine yields of each sampled population were determined throughout the simulated long-term cultivation. While an initial increase in relative L-cysteine yields of transformed W3110 strains towards a maximum was measured, the yields at 60 accumulated generations only reached 15–35% of the maximal product concentration. The cysteine yields of the W3110 strain with integrated pCYS\_i plasmid remained at a constant high level until a drop at 63 generations, while the other plasmids

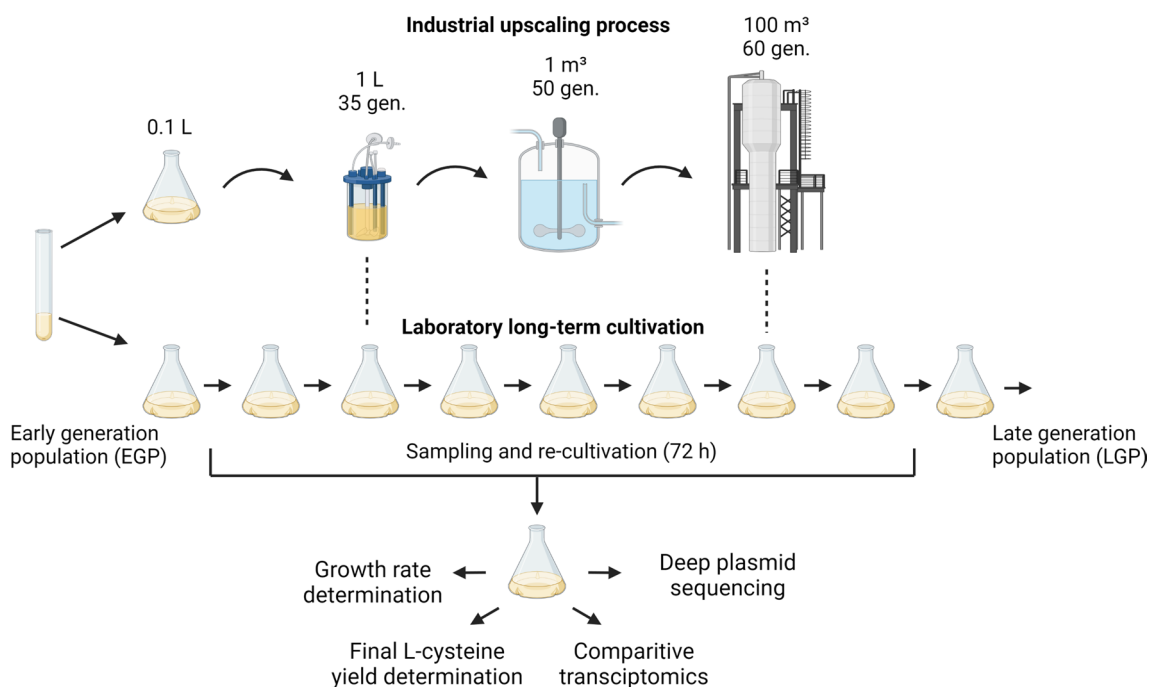


**Fig. 2** Laboratory long-term cultivation of L-cysteine producing *E. coli* cells. Adapted from Rugbjerg et al., 2018. One “wild-type” *E. coli* MG1655 strain (W3110) and a reduced genome strain (MDS42) were cultivated harbouring one out of three plasmid constructs (Fig. 1A). By serially transferring samples every 10 or 5 h into fresh medium, respectively, we imitate generation numbers found in large-scale industrial bioreactors. Thereby the cultures were kept in the exponential phase throughout the experiment. Sample collection was continued until desired generation numbers (>60) were achieved. Subsequently, all cryo-samples were re-cultivated for 72 h during which growth rate- and final L-cysteine yields were monitored. RNA extractions for comparative transcriptomics and plasmid extractions for deep plasmid sequencing were performed on the early and late generation population (EGP, LGP) samples for each strain and plasmid construct, respectively. Created with BioRender.com

showed a steady decline from generation 15–20 onwards (Fig. 3B). Transformed MDS42 strains showed no steady decline in generated L-cysteine yields with accumulating generations. Instead, the L-cysteine space time yields were stable at 75–100% (Fig. 3D). However, total L-cysteine yields in MDS42 populations were overall lower compared to W3110 populations (Additional file 1: Fig.S1). In case of the MDS42 strain, it should be taken into account that due to the deletion of 704 genes physiological differences exist in comparison to the W3110 strain. The effects depend on the biomolecule to be produced, when employing MDS42 as a cell factory.

Furthermore, we tested strain viability by determining growth rates of the sampled populations. As a function of generation numbers, growth rates of W3110 differed depending on the transformed plasmid (Fig. 3C). W3110 populations with integrated pCYS<sub>i</sub> plasmid showed no considerable changes in growth rate. In contrast, we observed a substantial change of fitness in case of W3110 with integrated pCYS<sub>m</sub> and pCYS. When comparing initial and final growth rates, we detected an increase of 13% for pCYS<sub>m</sub>, and 27% for pCYS. There was no considerable effect on fitness in transformed MDS42 populations (Fig. 3D).

Overall, the decline in L-cysteine yields tended to correlate with the increase in growth rates in an inversely proportional pattern, indicating an acquisition of fitness at the expense of L-cysteine production.

#### Transcriptome analyses reveals strong differences regarding expression levels in W3110 populations and few differences in MDS42 populations over the course of long-term cultivation

To determine potential causes for the collapse of L-cysteine production, we examined the transcriptomes of W3110 and MDS42 populations subjected to the long-term cultivation. We sequenced and compared transcriptomes from early generation populations (EGP) with later generation populations (LGP). Interestingly, when assessing global relationships between samples, we found that EGPs and LGPs of the MDS42 strains hardly differed from each other, while there were larger deviations in W3110 populations (Fig. 4). This result is consistent with previous findings of a limited evolutionary adaptability of the MDS42 strain and illustrates why we observed negligible changes in L-cysteine production and fitness in MDS42 populations [31, 32].

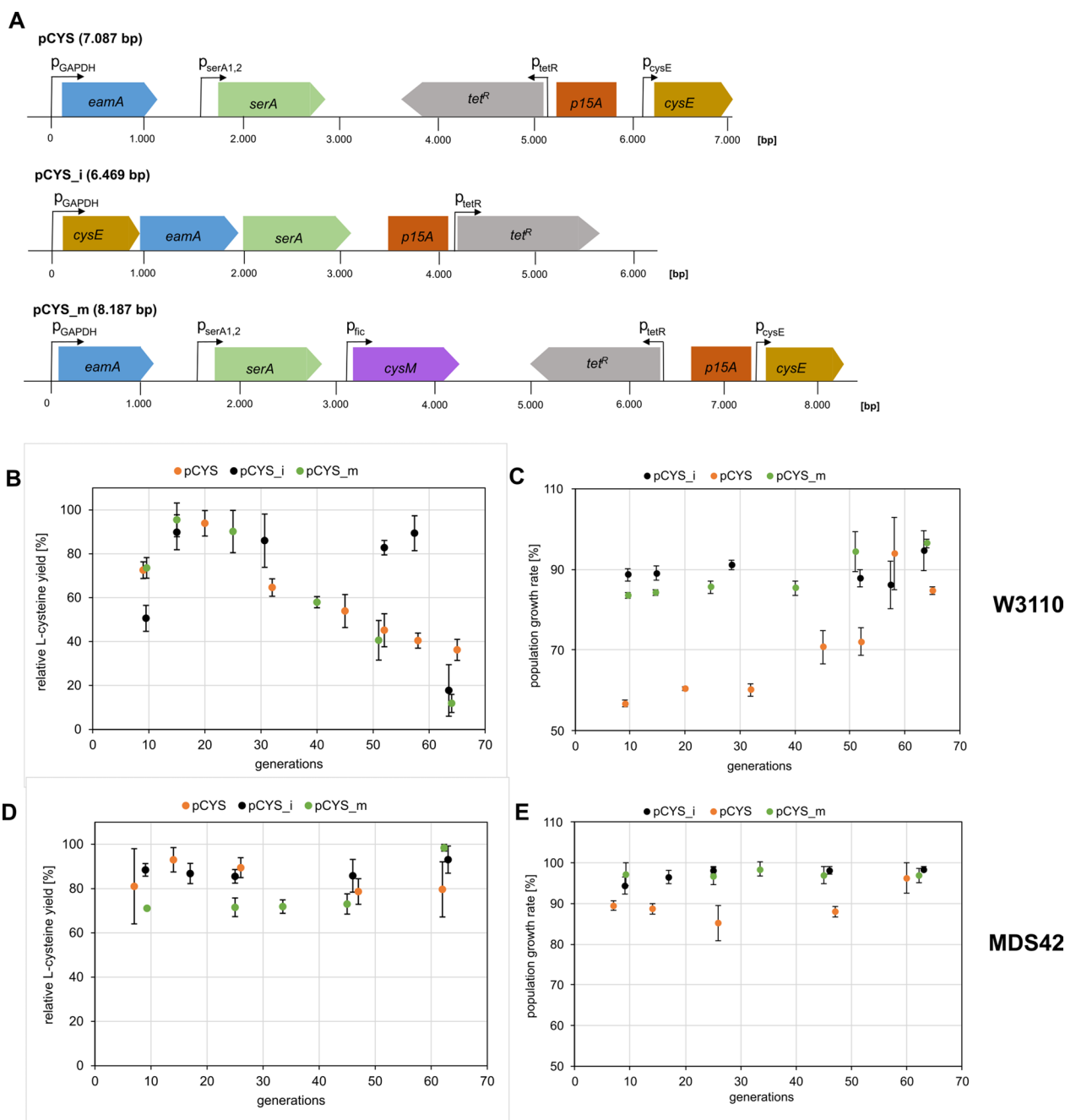


**Fig. 3** Stability of L-cysteine producing phenotypes. **A:** Plasmids used for transformation in *E. coli* W3110 and MDS42 to study the stability of L-cysteine production. Boxed arrows indicate genes located on the plasmid, whereas bended arrows display corresponding promoters. **B–E:** Plots of relative L-cysteine yields in % (B + D) and the population growth rates (C + E) as a function of accumulated generations. Cultivation and subsequent L-cysteine yield measurements were carried out in biological triplicates of W3110 and MDS42 with the three different plasmids shown in Fig. 3A. L-cysteine yields were normalised based on the OD<sub>600</sub> and the highest yield of the corresponding biological replicate (Additional file 1: fig. S1). Population growth rates were normalised based on growth rates of the corresponding non-producing strains harbouring empty vectors (Additional file 1: table S3)

**Metabolic clustering helps understanding the burden on cell populations during L-cysteine production**

To gain a deeper insight into the differences in expression

levels in W3110 and MDS42 populations, we examined differentially expressed genes (DEGs) with a p-value cut-off < 0.05 (Additional file 1: Tables S6–S11). After

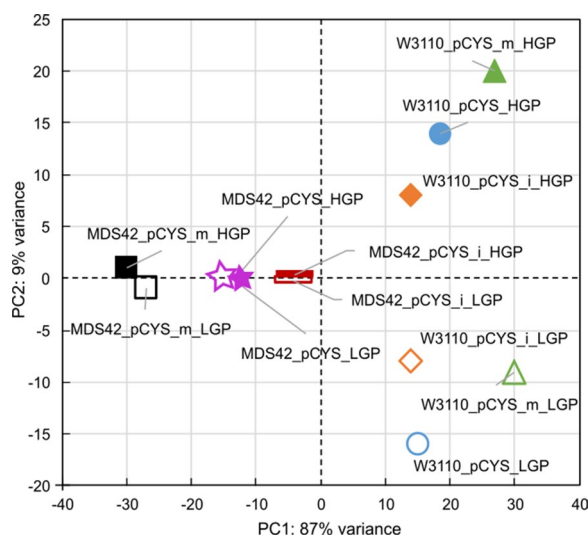


**Fig. 4** Principal component plot of all samples subjected to transcriptome analysis. Later generation populations (LGP) are marked with filled-in shapes, while shapes of early generation populations (EGP) are unfilled. LGPs correspond to populations with 60–65 evolved generations, while EGPs correspond to populations with 7–10 evolved generations. Related samples are marked with the same colour. Samples displayed in close proximity indicate very few differences between them while samples placed more distantly suggest bigger variations

clustering the DEGs according to their metabolic function, we subsequently plotted the number of DEGs in a cluster against the mean fold change of those in the cluster (Fig. 5). Overall, we noticed a lower number of different metabolic clusters in MDS42 populations than in W3110 populations. In general, stress features such as nitrogen starvation, acetyl-coA-, nitrate-, and carbon assimilation were up-regulated in EGPs, indicating a resource-draining L-cysteine production process. However, most up-regulated features in EGPs, where L-cysteine production was highest, belonged to the cluster of sulphur and L-cysteine starvation (Table 1). The metabolic flux towards L-cysteine coupled with overexpression of its corresponding exporter gene *eamA* most likely caused the intracellular deficiency of sulphur and the sulphuric amino acid.

In LGPs, additionally to up-regulated clusters such as biofilm formation, iron starvation and anaerobic respiration, we also identified features belonging to an L-cysteine degradation operon (Table 2). The corresponding D/L-serine membrane transporter CyuP was potentially protecting the cell from increasing sulphur starvation by shuttling serine out of the cell before this precursor amino acid was further metabolised to L-cysteine. CyuA, on the other hand, may have acted as an L-cysteine desulfidase releasing sulphur by degradation for cell homeostasis. The observation of the decrease

in measured L-cysteine yields in LGPs supports this hypothesis. Furthermore, we suspected that the expression of the *cyuAP* operon was triggered by sulphur starvation.

Additionally, it would be worth to consider adding the transcription factor *cysB* into the plasmid construct, therefore enhancing sulphur utilisation and sulfonate-sulfur catabolism via L-cysteine production. Recombinant expression of *cysB* has been demonstrated to enhance L-cysteine yields in *E. coli* [33].

In the further course of the transcriptome analysis, we found clusters that indicated genetic instability of the production strains. Transposases for insertion sequence families 3 and 66 as well as mismatch repair genes were upregulated in LGPs (Table 2). In the sulphur and L-cysteine starvation cluster of EGPs we detected *cysD*, a gene that facilitates stress-induced mutagenesis (SIM) [34]. Therefore, we examined the impact of this genetic instability on the plasmid level.

#### Deep sequencing reveals an accumulation of insertion sequences (IS) in production plasmids of evolving populations

When calculating and comparing the contents of extracted plasmids per  $\mu\text{g}$  cells of EGPs and LGPs, we observed no relevant differences (Additional file 1: Table S12). The L-cysteine production decline could therefore not be linked to lower plasmid quantities in LGPs. In a next step, we deep sequenced plasmids from EGPs and LGPs and mapped the sequenced reads against the associated plasmid sequence reference (Methods). The average per base coverage depth was  $>140.000\times$  (Additional file 1: Fig. S2–S4). Consistent with other studies, we did not find genetic variance in plasmid genes by single nucleotide polymorphism (SNP) analyses (Additional file 1: Table. S13), [20, 21]. Interestingly, we noticed an increase in unmapped reads in LGPs of W3110 compared to EGPs (Fig. 6A). In a next step, we mapped these reads against an insertion sequence database from *E. coli* revealing higher coverages of aligned reads to IS in LGPs (Fig. 6A). Surprisingly, we also identified reads, that could be mapped to IS in plasmids from MDS42 populations, although the number was reduced by tenfold. In order to assign the mapped reads to the different IS families, we used NCBI's megablast algorithm (Methods).

The distribution of the different IS families was very similar for all three production plasmids. This observation was the same for EGPs compared to LGPs (Fig. 6B). Nevertheless, the total number of reads that could be mapped to IS doubled on average when comparing W3110 EGPs with LGPs, while the number remained the same for MDS42 populations. This indicates, that transpositions of different IS families propagated in similar

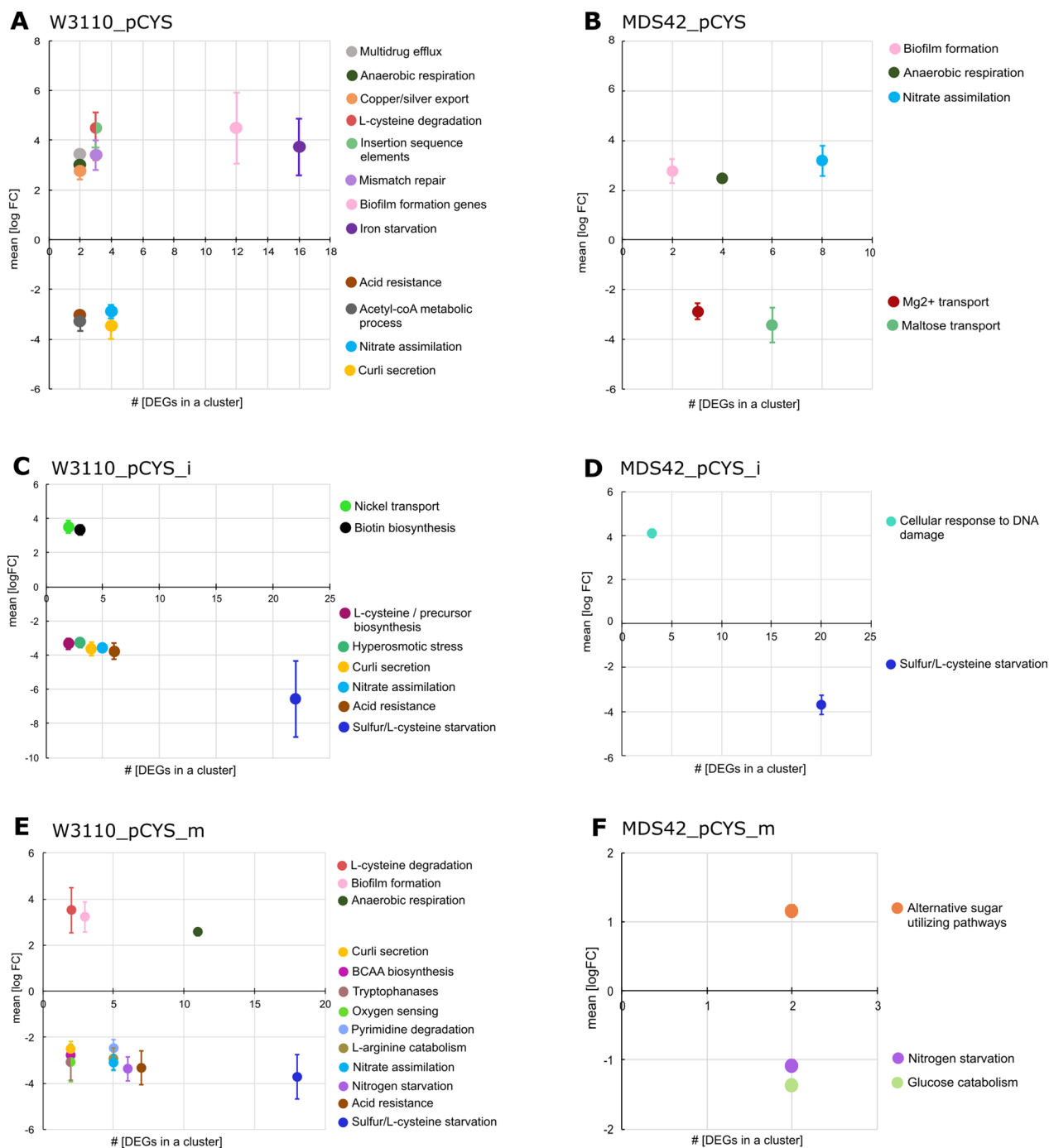


**Fig. 5** Clustering of differentially expressed genes (DEGs) based on the metabolic function in *E. coli*. For this, logarithmic fold change (logFC) medians of DEGs with the same metabolic function were plotted against the number of DEGs within this group. Fold changes were calculated by dividing values of the later generation population (LGP) by values of the early generation population (EGP). LGPs correspond to populations with 60–65 evolved generations, while EGPs correspond to populations with 7–10 evolved generations. *E. coli* strains W3110 (A, C, E) and MDS42 (B, D, F) transformed with one of three plasmids engineered for L-cysteine production (pCYS: A, B; pCYS\_i: C, D; pCYS\_m: E, F) were analysed. A p-value cut-off < 0.05 was selected. Genes with unknown function as well as clusters mapped with only one gene were disregarded here, but can be found in Additional file 1: Tables S6-S11. **A:** 81 genes in total (57 genes within 12 cluster, 20 genes with unknown function and 4 single gene clusters). **B:** 34 genes in total (34 genes within 5 cluster, 6 genes with unknown function and 2 single gene clusters). **C:** 65 genes in total (47 genes within 8 cluster, 10 genes with unknown function and 8 single gene clusters). **D:** 23 genes within 2 cluster. **E:** 105 genes in total (70 genes within 12 cluster, 17 genes with unknown function and 18 single gene clusters). **F:** 14 genes in total (6 genes within 3 cluster, 4 genes with unknown function and 4 single gene clusters)

**Table 1** List of sulphur and L-cysteine metabolism related operons detected as clusters in transcriptome analysis

DEGs of sulphur/ L-cysteine metabolism related operons	Metabolic function	Literature
<i>cyuAP</i>	L-cysteine desulfidase, L-cysteine utilization permease	[35], [36]
<i>asIB</i>	Putative anaerobic sulfatase maturation enzyme	[37]
<i>tauABCD</i>	Taurine utilization proteins	[38]
<i>ssuEADCB</i>	Aliphatic sulfonates utilization proteins	[39]
<i>cysPUWA, sbp</i>	Sulphate/thiosulphate transport proteins	[40], [41]
<i>cysDNC</i>	Sulphate activation proteins	[42]
<i>cysJIH</i>	Sulphite reductase proteins	[43]
<i>tsuAB</i>	Thiosulphate transport proteins	[44]

**Table 2** List of genes related to genetic instability detected in transcriptome analysis

DEGs belonging to genetic instability	Metabolic function	Literature
<i>insJK</i>	IS3 family transposase	[45]
<i>yjgZ</i>	Putative IS66 family transposase	InterPro
<i>ybcN, rusA, iprA</i>	DNA repair	[46], [47], [48]

frequencies. For plasmids extracted from W3110 populations, we most frequently identified reads that could be mapped to the IS3 and IS5 family, which supports the result of a high expression of *insJK*, an IS3 family transposase, in LGPs of W3110\_pCYS. In addition, reads mapped to the ISAs1 family were very abundant. Among plasmids from MDS42 populations, the reads could be mapped mainly to sequences belonging to IS200- and IS110 families. Due to deletion of most IS, the few transposition events in MDS42 populations are in line with the stable L-cysteine production and growth rates, rendering *E. coli* MDS42 as a stable host for industrial L-cysteine fermentations.

## Conclusions

The data in this study suggest that insertion sequence (IS) transposition, triggered by the metabolic stress of L-cysteine production, leads to structural genetic rearrangements in production plasmids. Within 60 generations, as achieved in industrial large-scale fermentations, L-cysteine production capacities collapsed by up to 65–85% in *E. coli* W3110 populations while growth rates increased up to 27% depending on the L-cysteine plasmid construct. Contrarily, *E. coli* MDS42 populations exhibited nearly stable space–time yields of 75–100% with no considerable effect on growth related fitness.

Metabolic stress of L-cysteine producing populations, cultivated in shake flasks, as illustrated in this study, certainly differs from cultures grown in large-scale bioreactors, e.g. O<sub>2</sub> limitation as reflected in upregulation

of anaerobic genes in LGPs. Yet the fundamental issue is the same: Cells are driven to eliminate factors that impair growth fitness by evolutionary adaptation. Frequently, these factors involve metabolically burdensome compounds meant to be produced by engineered *E. coli* cells, establishing non-producing populations in continuous cultivations [21, 49–52].

Common industrial practice employs clone banks of production strains stored as frozen aliquots. Although the population appears inconspicuous for a number of divisions, a few cells present in the starting seed may harbour genetic mutations. Cell bank aliquots with rare pre-existing mutations that disrupt production, should therefore be screened beforehand, using deep-sequencing techniques.

Opposed to previous work relying on PCR-based methods for IS identification, we chose a deep sequencing approach on population level circumventing amplification biases [53]. Thereby, an accumulation of predominantly IS3 and IS5 fragments could be detected in W3110 LGPs, whereas IS accumulation was neglectable in MDS42 populations. However, due to read length limitations of the Illumina sequencing technology, mapping of IS to the corresponding plasmid reference sequences pose a hindrance. In addition, repetitive sequences within IS complicate distinguishability and read assembly. For this purpose, the Burrows-Wheeler aligner's Smith-Waterman alignment (BWA-SW) is suitable to capture chimeric reads containing junctions between plasmid and IS sequences with frequent alignment gaps. From a future perspective, we suggest the usage of long read sequencers such as PacBio or Oxford Nanopore for a deeper understanding of IS mediated transposition into plasmid sequences. Full coverage of singular plasmid sequences would provide both the full length IS and its insertion site.

Consequently, the genetically stable minimal genome *E. coli* strain MDS42 rendered as a promising host for L-cysteine production. However, MDS42, while



**A**

Plasmid	pCYS				pCYS_i				pCYS_m			
	W3110		MDS42		W3110		MDS42		W3110		MDS42	
Strain	EGP	LGP	EGP	LGP	EGP	LGP	EGP	LGP	EGP	LGP	EGP	LGP
Unmapped reads to plasmid sequence [%]	4.4	8.2	2.7	2.5	3.3	6	2.5	2.4	3.8	7.1	2	2.1
Reads mapped to IS [%]	0.13	0.24	0.01	0.01	0.11	0.18	0.01	0.01	0.12	0.23	0.01	0.01
Reads mapped to IS [total]	3803	5852	271	249	2361	5253	261	245	2101	6070	180	196

**B**

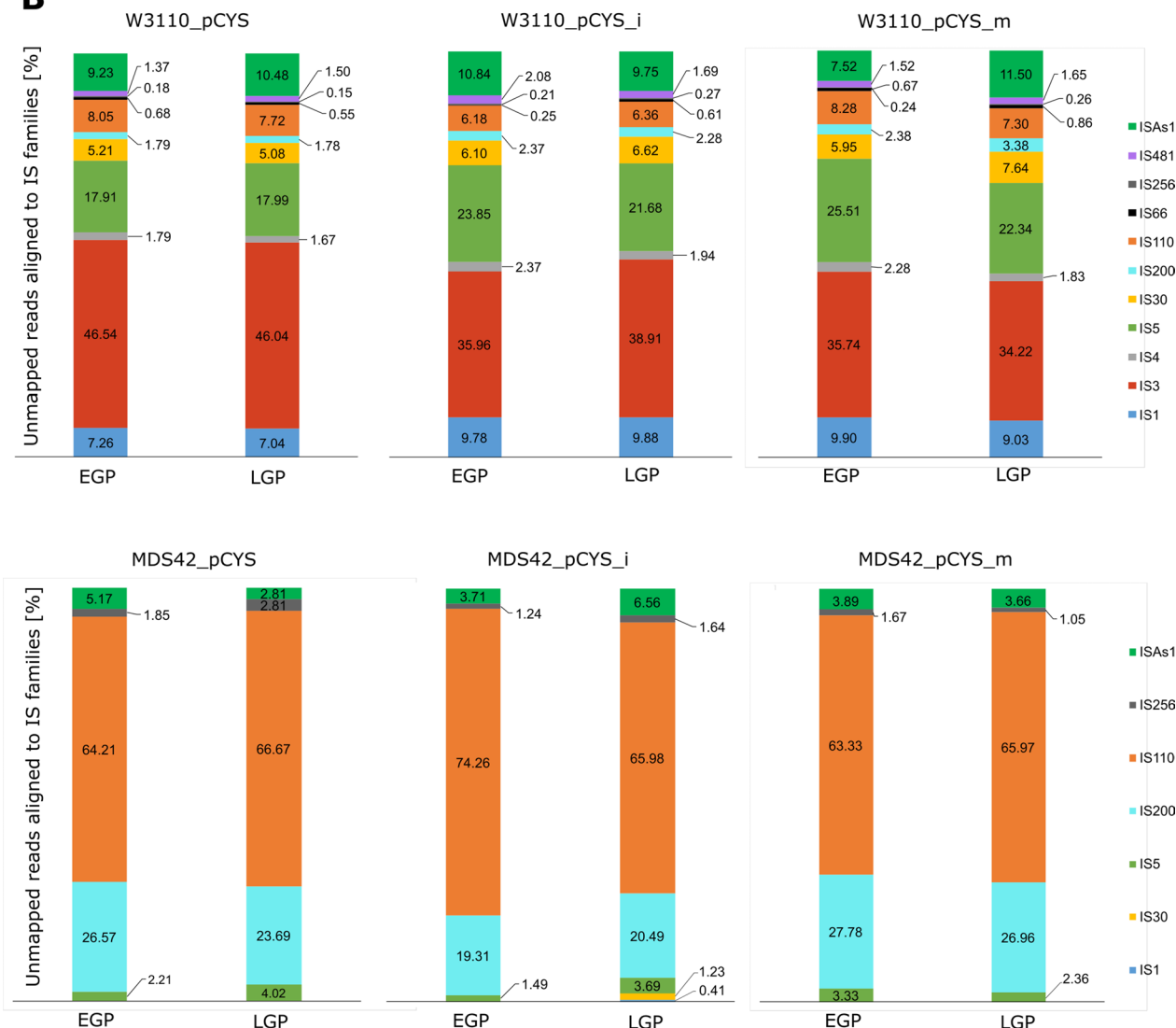


**Fig. 6** Mapping of sequenced reads against insertion sequence (IS) families. **A:** Table showing the percentages of reads that did not map to the plasmid sequences as well as the percentages of those unmapped reads mapped to IS. Plasmids pCYS, pCYS\_i and pCYS\_m extracted from early and late generation populations of W3110 and MDS42 got deep sequenced (Methods). **B:** Proportions of unmapped reads aligned to the different IS families in percent. The caption is arranged in the same order as the stacked bars

showing a superior growth rate and stability compared to W3110, exhibits an overall lower L-cysteine space-time yield (Additional file 1: Fig. S1).

This study postulates that selective deletion of IS and the corresponding transposases in genomes of industrially relevant production strains, such as W3110 can be

used as a new, more-targeted approach to optimise the *E. coli* based industrial L-cysteine production. This could provide a trade-off between increased plasmid stability over the entire production phase while maintaining evolutionary adaptability of the cell system linked to high cell density fermentations at maximal growth rates and L-cysteine productivity.

## Materials and methods

### Strains and plasmids

Two parental *E. coli* K12 strains were used to construct the strains with three specific plasmids (Table 3):

*E. coli* W3110: *F-λ-rph-1 INV(rrnD, rrnE)*.

*E. coli* MDS42 (Scarab Genomics): MG1655 genome almost free from any ISs, *fhuACDB, endA* and more [48].

For introduction of the plasmids into the strains, standard transformations with chemical competent cells were performed. For the long-term cultivation experiments, single colonies of freshly transformed cells were used to inoculate precultures.

PCYS\_i was generated by ligation of four amplified and digested amplicons in an equimolar ratio in a 40 μl reaction. The fragments contained the metabolic pathway genes of pCYS (*ydeD, cysE-XIV* and *serA317*) and the empty vector as a backbone. The digestions were conducted with SacI, XhoI, BamHI, PacI, and NcoI. Fast digest restriction enzymes, buffer, the T4 DNA Ligase as well as the Phusion DNA polymerase were used from Thermo Fisher Scientific. For amplification of different fragments, specific PCR primer were used (Additional file 1: Table S1). PCYS\_m was generated by introducing the stationary phase promoter *pfic* and the *cysM* gene into the backbone of pCYS via Gibson cloning standard procedure (NEB). PCRs were performed with specifically designed primers (Additional file 1: Table S1).

### Media

A custom cultivation medium for the production of L-cysteine was used for all cultivations. This medium consisted of 10 g/L glucose, 5 g/L KH<sub>2</sub>PO<sub>4</sub>, 5 g/L (NH<sub>4</sub>)<sub>2</sub>SO<sub>4</sub>, 1 g/L Na<sub>3</sub>Citrat × 2 H<sub>2</sub>O, 0.9 g/L L-isoleucine, 0.6 g/L D, L-methionine, 0.5 g/L NaCl, 2 g/L ammonium thiosulphate, 1.2 g/L MgSO<sub>4</sub> × 7 H<sub>2</sub>O, 18 mg/L thiamine-HCl, 9 mg/L pyridoxine-HCl, 15 mg/L tetracycline and

100 ml/L LB-medium. Additionally, 10 ml/L of a trace element solution was added. This trace element solution included 3.75 g/L H<sub>3</sub>BO<sub>4</sub>, 1.55 g/L CoCl<sub>2</sub> × 6 H<sub>2</sub>O, 0.55 g/L CuSO<sub>4</sub> × 5 H<sub>2</sub>O, 3.55 g/L MnCl<sub>2</sub> × 4 H<sub>2</sub>O, 0.65 g/L ZnSO<sub>4</sub> × 7 H<sub>2</sub>O, and 0.33 g/L Na<sub>2</sub>MoO<sub>4</sub> × 2 H<sub>2</sub>O. The trace element solution is adjusted to pH 4.0 with HCl before autoclaving. Everything else got sterile filtrated after pH adjustment to 7–7.05. Tetracycline, vitamins, CaCl<sub>2</sub> and MgSO<sub>4</sub> were added immediately before inoculation.

### Simulated long-term cultivation

The simulated long-term cultivation method was adapted from Rugbjerg et al. [21]. Single colonies of freshly transformed cells were inoculated into 250 ml baffled shaking flasks containing 25 ml medium. W3110 strains were cultivated at 32 °C for 10 h and horizontal shaking at 150 r.p.m (New Brunswick Innova 44). Each strain harbouring one out of three plasmids got cultivated in triplicates. Due to a higher growth rate of the MDS42 strain, cultures were kept at 32 °C just for 5 h to always maintain an exponential growth phase. After each time point cultures were inoculated into 25 ml fresh medium (starting OD<sub>600</sub> = 0.05) and incubated under the same conditions for another 10 h or 5 h. At each passage, sample's OD<sub>600</sub> were recorded to determine the accumulated generations (Additional file 1: Table S2) and 1 ml got snap-frozen with 1 ml 50% glycerol in liquid N<sub>2</sub> and stored at – 80 °C. Subsequently the sampled cryo-cultures were re-cultivated for 72 h with a starting OD<sub>600</sub> of 0.01 into 25 ml fresh medium under above mentioned conditions. Growth rates were monitored every 30 min. L-cysteine yield determination was performed after 72 h. RNA extraction was carried out at OD<sub>600</sub> values of 0.6–0.8. Extraction of plasmid DNA was performed from the same culture (Fig. 2).

### Determination of L-cysteine yields by spectrophotometry

Each population sample from the glycerol stock was used for inoculation of 25 ml medium and the culture got cultivated at 32 °C at 150 r.p.m for 72 h (New Brunswick Innova 44). After incubation, 1 ml culture was centrifuged at 15.000 × g for 1 min. Both the pellet and the supernatant were further treated according to a modified

**Table 3** Plasmids used in this study: All plasmids are derived from pACYC184 with a p15A origin of replication and approx. 15 copies/cell

Plasmid	Relevant features	References
pCYS	P <sub>GAPDH</sub> : <i>ydeD</i> , P <sub>serAp1,2</sub> : <i>serA317</i> , p <sub>cysE</sub> : <i>cysE-XIV</i> , tet <sup>R</sup> , p15A	[26, 27, 29, 30]
pCYS_i	P <sub>GAPDH</sub> : <i>cysE-XIV-ydeD-serA317</i> , tet <sup>R</sup> p15A	This study
pCYS_m	P <sub>GAPDH</sub> : <i>ydeD</i> , P <sub>serAp1,2</sub> : <i>serA317</i> , p <sub>fic</sub> : <i>cysM</i> , p <sub>cysE</sub> : <i>cysE-XIV</i> , tet <sup>R</sup> , p15A	This study

method of Gaitonde to determine the L-cysteine yields (Additional file 1: Note 1) [54].

### Measurement of population growth rates

In order to measure population growth rates, the OD<sub>600</sub> values of cultures grown for L-cysteine productivity analysis (as described in the previous section) were recorded every hour. Un-inoculated medium was used for background subtraction. Calculation of growth rates were performed with the following formula:

$$r = \frac{N(t)^{\frac{1}{t}}}{N(0)} - 1$$

where: N(t): cell number at time t, N (0): cell number at time 0, r: growth rate and t: time passed. Values of measured growth rates can be found in Additional file 1: Table S3. Population growth rates were normalised based on growth rates of the corresponding non-producing strains harbouring empty vectors.

Cell number counts were calculated with Agilent's online tool "E. coli Cell Culture Concentration from OD<sub>600</sub> Calculator" (<https://www.agilent.com/store/biocalculators/calcODBacterial.jsp>, accessed 11/14/2022).

### RNA sequencing and analysis

Sampled cryo-cultures of the simulated long-term cultivation were re-cultivated for 72 h with a starting OD<sub>600</sub> of 0.01 into 25 ml fresh medium under above mentioned conditions. One sample per early/late generation population, plasmid and strain (12 in total; strains: W3110, MDS42; plasmids: pCYS, pCYS\_i, pCYS\_m) were chosen for RNA extractions using a standard RNA extraction kit (Promega SV total RNA isolation system). Depletion of ribosomal RNA, transcriptome library construction, and sequencing of the corresponding samples were performed by Eurofins Genomics. Sequencing was conducted with the technology of Illumina NovaSeq 6000 with a 150 bp paired-end reading. Raw read counts were created using featureCounts (version 1.5.1) [55]. Only reads overlapping "CDS" features were counted. All reads mapping to features with the same meta-feature attribute were summed. Only reads with unique mapping positions and a mapping quality score of at least 10 were considered for read counting. Supplementary alignments were ignored. Instead of counting paired-end reads twice, they were counted only once, i.e. as single fragment. Reads mapping to multiple features were assigned to the feature that has the largest number of overlapping bases. A Trimmed Mean of M-values (TMM) normalization was performed using the edgeR package (version 3.16.5)

[56, 57]. Mapping of reads to reference sequences of *E. coli* K-12 W3110 and *E. coli* K-12 MDS42 was performed using BWA-NEM (version 0.7.12-r1039).

To determine which features are significantly differentially expressed, a small threshold (<<0.01) was applied to the false discovery rate (FDR) values, which is the p-value adjusted for multiple testing using Benjamini–Hochberg procedure. Fold changes were calculated by dividing values of the later generation population (LGP) by values of the early generation population (EGP).

The metabolic gene clustering was carried out with the EcoCyc *E. coli* database regarding all differentially expressed features with p-values < 0.05. Mapping results and expression profiling statistics are shown in Additional file 1: Tables S4, S5.

### Plasmid analysis of early and late generation population of E. coli W3110 and MDS42

Sampled cryo-cultures of the simulated long-term cultivation were re-cultivated for 72 h with a starting OD<sub>600</sub> of 0.01 into 25 ml fresh medium under above mentioned conditions. One sample per early/late generation population, plasmid and strain (12 in total; strains: W3110, MDS42; plasmids: pCYS, pCYS\_i, pCYS\_m) were chosen for plasmid extraction, using a standard kit (ThermoFisher Scientific GeneJET Plasmid Miniprep Kit). In order to test for potential plasmid loss during cultivation, we determined the plasmid DNA content in early and late generation populations (Additional file 1: Table S12). For the subsequent library preparation and deep sequencing was performed by Eurofins Genomics for Illumina NovaSeq 6000 S4 paired-end 2 × 150 bp. The per base coverage depth was > 140,000x. Adapter trimming, quality filtering and per-read pruning was done to retain only high quality bases. Reads were then mapped to the corresponding reference plasmid sequence, followed by a single nucleotide variant calling. Reads which could not be mapped to the plasmid reference sequences, got then mapped against an insertion sequence database (ISfinder\_Nucl) with the Burrows-Wheeler Aligner. The reads, which could then be mapped to insertion sequences, were blasted against each insertion sequence family in the *E. coli* W3110 genome with NCBI's megablast algorithm. Only highly similar sequences were selected and displayed.

### Abbreviations

ALE	Adaptive laboratory evolution
<i>C. Glutamicum</i>	<i>Corynebacterium glutamicum</i>
DEG	Differentially expressed gene
<i>E. coli</i>	<i>Escherichia coli</i>
EGP	Early generation population
IS	Insertion sequence
LGP	Late generation population

NGS	Next generation sequencing
R.P.M	Rounds per minute
SNP	Single-nucleotide polymorphism

## Supplementary Information

The online version contains supplementary material available at <https://doi.org/10.1186/s12934-023-02021-5>.

**Additional file 1: Table S1.** Oligo sequences used for assembly of plasmids pCYS\_i and pCYS\_m. **Table S2.** Average number of generations after each passage of the simulated fermentation of W3110 and MDS42 with integrated pCYS, pCYS\_i and pCYS\_m. Each strain was cultivated in biological triplicates. **Table S3.** Average growth rates of samples taken after each passage of the simulated long-term cultivation of W3110 and MDS42 with integrated pCYS, pCYS\_i and pCYS\_m. Each strain was cultivated in biological triplicates. Growth rates were calculated according to the formula found in the manuscripts' methods section of "Measurement of population growth rates". **Table S4.** Mapping statistics overview. For each sample, the following statistics are provided: Reads mapped: the total number of reads mapped to the reference genome. Unique: number of uniquely mapped reads, i.e. read can only be mapped to one reference locus. Reference covered: reference bases covered by at least one read. Mean read coverage: average read coverage of the reference sequence. HGP: high generation population, LGP: low generation population. **Table S5.** Expression profiling statistics. For each sample, the following statistics are provided: Effective library size: The total number of reads mapped to reference features. Normalized library size: The total number of reads mapped to reference features normalized by the associated normalization factor, which can be derived by dividing the normalized library size by the effective library size. No feature: The number of reads mapping to the reference sequence that could not be assigned to any annotated feature, i.e. mapping positions and feature positions do not overlap. Filtered: The number of reads that were filtered due to insufficient mapping quality or ambiguous mapping location. These reads were ignored for read counting. **Table S6.** Table showing accession numbers, gene names, features, logarithmic fold changes (logFC) and p-values of all differentially expressed genes (DEGs) of W3310\_pCYS with p-values <0.05. LogFC and logCPM were calculated by dividing values of the later generation population (LGP) by values of the early generation population (EGP). \*: Genes were excluded because they did not fall within the FC range of the metabolic cluster. **Table S7.** Table showing accession numbers, gene names, features, logarithmic fold changes (logFC) and p-values of all differentially expressed genes (DEGs) of MDS42\_pCYS with p-values <0.05. LogFC and logCPM were calculated by dividing values of the later generation population (LGP) by values of the early generation population (EGP). **Table S8.** Table showing accession numbers, gene names, features, logarithmic fold changes (logFC) and p-values of all differentially expressed genes (DEGs) of W3110\_pCYS\_i with p-values <0.05. LogFC and logCPM were calculated by dividing values of the later generation population (LGP) by values of the early generation population (EGP). **Table S9.** Table showing accession numbers, gene names, features, logarithmic fold changes (logFC) and p-values of all differentially expressed genes (DEGs) of MDS42\_pCYS\_i with p-values <0.05. LogFC and logCPM were calculated by dividing values of the later generation population (LGP) by values of the early generation population (EGP). **Table S10.** Table showing accession numbers, gene names, features, logarithmic fold changes (logFC) and p-values of all differentially expressed genes (DEGs) of W3110\_pCYS\_m with p-values <0.05. LogFC and logCPM were calculated by dividing values of the later generation population (LGP) by values of the early generation population (EGP). **Table S11.** Table showing accession numbers, gene names, features, logarithmic fold changes (logFC) and p-values of all differentially expressed genes (DEGs) of MDS42\_pCYS\_m with p-values <0.05. LogFC and logCPM were calculated by dividing values of the later generation population (LGP) by values of the early generation population (EGP). **Table S12.** Values of calculated plasmid DNA contents extracted from early and late generation populations (EGP, LGP). Plasmid DNA was extracted from 10 ml cultures and eluted in 50 µl each. Cell dry weights were extrapolated with the factor of 0.33 g/L/OD<sub>600</sub>=1.0 for *E. coli* K-12 MG1655 cells according to Sauer et al. (2). **Table S13.** Single-nucleotide

polymorphism (SNP) variant table. The SNP calling was done using VarScan2 (3). Allele frequency cut-off used for variant calling was 1%. For each sample, the following variant summary is provided: Strain, plasmid, population. Additionally, POS: Position at which the variant was observed, BB/ORF: Location affected by the mutation (BB: backbone, ORF: open reading frame), REF: Reference base, ALT: Alternative base, Allele Freq: Variant allele frequency in percentage, Alt Depth: Depth of variant-supporting bases, total depth: Depth of variant-supporting bases and reference-supporting bases. Mutations which showed allele-frequencies >95% were assumed to be originally present in the plasmids. **Figure S1.** Plots of total L-cysteine yields in mg/OD<sub>600</sub> = 1.0. Cultivation and subsequent L-cysteine yields determination was carried out in biological triplicates of W3110 (A) and MDS42 (B) with the three different plasmids pCYS, pCYS\_i and pCYS\_m. **Figure S2.** Per base coverage depths (x) of sequenced pCYS extracted from early and late generation populations (EGPs and LGPs) of *E. coli* W3110 and MDS42. Sequencing was conducted with Illumina Novaseq paired end 2x150bp. **Figure S3.** Per base coverage depths (x) of sequenced pCYS\_i extracted from early and late generation populations (EGPs and LGPs) of *E. coli* W3110 and MDS42. Sequencing was conducted with Illumina Novaseq paired end 2x150bp. **Figure S4.** Per base coverage depths (x) of sequenced pCYS\_m extracted from early and late generation populations (EGPs and LGPs) of *E. coli* W3110 and MDS42. Sequencing was conducted with Illumina Novaseq paired end 2x150bp. **Note 1.** Spectrophotometric protocol for L-Cysteine determination adapted from Gaitonde (1).

### Acknowledgements

Not applicable

### Author contributions

TBB: Funding acquisition, Project administration, Conceptualisation, Writing-Reviewing & Editing KH: Conceptualization, Methodology, Investigation, Data curation, Writing—Original draft preparation and reviewing & editing NDA: Investigation, Writing—Reviewing & Editing. TB and KH conceived and designed the study. KH carried out the experiments and drafted the manuscript. KH, NA and TB edited and finalised the manuscript. All authors read and approved the final manuscript.

### Funding

Open Access funding enabled and organized by Projekt DEAL. The study was financed by the industrial Contract No #2018112610005964.

### Availability of data and materials

All data and materials are available as described in the study and its additional Additional file 1.

### Declarations

#### Ethics approval and consent to participate

Not applicable.

#### Consent for publication

Not applicable.

#### Competing interests

There are no conflicts to declare.

Received: 20 October 2022 Accepted: 9 January 2023

Published online: 16 January 2023

### References

- Cicchillo RM, Baker MA, Schnitzer EJ, Newman EB, Krebs C, Booker SJ. *Escherichia coli* L-serine deaminase requires a [4Fe-4S] cluster in catalysis. *J Biol Chem.* 2004;279(31):32418–25.

2. Johnson DC, Dean DR, Smith AD, Johnson MK. Structure, function, and formation of biological iron-sulfur clusters. *Annu Rev Biochem.* 2005;74:247–81.
3. Barrose JM. Commission Implementing Regulation (EU) No 1006/2013 concerning the authorisation of L-cysteine as a feed additive for all animal species. *Official J European Union.* 2013;59–60.
4. Clemente Plaza N, Reig Garcia-Galbis M, Martinez-Espinosa RM. Effects of the usage of L-Cysteine (L-Cys) on human health. *Molecules.* 2018. <https://doi.org/10.3390/molecules23030575>.
5. Ismail NI. Production of cysteine: approaches, challenges and potential solution. *Int J Biotechnol Wellness Indus.* 2014;3:95–101.
6. Renneberg R. High grade cysteine no longer has to be extracted from hair. *Biotechnology for beginners.* Amsterdam: Academic Press; 2008. p. 132.
7. Berehoiu RMT, Popa CN, Popescu S. Assessment of the E 920 additive (L-cysteine) in relation to some problems of modern food industry. *Economic Eng Agric Rural Devel.* 2013;13(1):413–8.
8. Shiba T, Takeda K, Yajima M, Tadano M. Genes from *Pseudomonas sp.* strain BS involved in the conversion of L-2-amino-Delta(2)-thiazolin-4-carbonic acid to L-cysteine. *Appl Environ Microbiol.* 2002;68(5):2179–87.
9. Nam KH. Effects of anoxic conditions on the enzymatic conversion of D, L-2-amino-thiazoline-4-carboxylic acid to L-cysteine. *Acta Biotechnol.* 1997;17:185–93.
10. Wei L, Wang H, Xu N, Zhou W, Ju J, Liu J, et al. Metabolic engineering of *Corynebacterium glutamicum* for L-cysteine production. *Appl Microbiol Biotechnol.* 2019;103(3):1325–38.
11. Nielsen J, Keasling JD. Engineering cellular metabolism. *Cell.* 2016;164(6):1185–97.
12. Borkowski O, Ceroni F, Stan GB, Ellis T. Overloaded and stressed: whole-cell considerations for bacterial synthetic biology. *Curr Opin Microbiol.* 2016;33:123–30.
13. Carbonell-Ballester M, Garcia-Ramallo E, Montanez R, Rodriguez-Caso C, Macia J. Dealing with the genetic load in bacterial synthetic biology circuits: convergences with the Ohm's law. *Nucleic Acids Res.* 2016;44(1):496–507.
14. Lynch M, Marinov GK. The bioenergetic costs of a gene. *Proc Natl Acad Sci USA.* 2015;112(51):15690–5.
15. Ceroni F, Algar R, Stan GB, Ellis T. Quantifying cellular capacity identifies gene expression designs with reduced burden. *Nat Methods.* 2015;12(5):415–8.
16. Glick BR. Metabolic load and heterologous gene expression. *Biotechnol Adv.* 1995;13:247–61.
17. Matthew Scott CWG, Mateescu Eduard M, Zhang Zhongge, Hwa Terence. Interdependence of cell growth and gene expression, origins and consequences. *Science.* 2010;330:1099–102.
18. Ohtsu I, Wiriyathanawudhiwong N, Morigasaki S, Nakatani T, Kado-kura H, Takagi H. The L-cysteine/L-cystine shuttle system provides reducing equivalents to the periplasm in *Escherichia coli*. *J Biol Chem.* 2010;285(23):17479–87.
19. Susann Müller HHaTB. Origin and analysis of microbial population heterogeneity in bioprocesses. *Anal Biotechnol.* 2010;21:100–13.
20. Xiao Y, Bowen CH, Liu D, Zhang F. Exploiting nongenetic cell-to-cell variation for enhanced biosynthesis. *Nat Chem Biol.* 2016;12(5):339–44.
21. Ruggberg P, Myling-Petersen N, Porse A, Sarup-Lytzen K, Sommer MOA. Diverse genetic error modes constrain large-scale bio-based production. *Nat Commun.* 2018;9(1):787.
22. Podlesek Z, Zgur BD. The DNA damage inducible SOS response is a key player in the generation of bacterial persister cells and population wide tolerance. *Front Microbiol.* 2020;11:1785.
23. Napolitano R, Janel-Bintz R, Wagner J, Fuchs RP. All three SOS-inducible DNA polymerases (Pol II, Pol IV and Pol V) are involved in induced mutagenesis. *EMBO J.* 2000;19:6259–65.
24. Löffler M, Simen JD, Jäger G, Schaferhoff K, Freund A, Takors R. Engineering *E. coli* for large-scale production—strategies considering ATP expenses and transcriptional responses. *Metab Eng.* 2016;38:73–85.
25. Harder BJ, Bettenbrock K, Klamt S. Model-based metabolic engineering enables high yield itaconic acid production by *Escherichia coli*. *Metab Eng.* 2016;38:29–37.
26. Leinfelder W, Heinrich P. European Patent Office. Process for preparing O-Acetylserine, L-cysteine and L-cysteine-related products. EP0858510B1 (Patent) 2001.
27. Bell JK, Pease PJ, Bell JE, Grant GA, Banaszak LJ. De-regulation of D-3-phosphoglycerate dehydrogenase by domain removal. *Eur J Biochem.* 2002;269(17):4176–84.
28. Daßler T. Identification of a major facilitator protein from *Escherichia coli* involved in efflux of metabolites of the cysteine pathway. *Mol Microbiol.* 2000;36:1101–12.
29. Winterhalter C, Leinfelder W. European Patent Office. Microorganisms and process for the fermentative production of L-Cysteine, L-Cystine, N-Acetyl-Serine or thiazolidin-derivates. EP0885962B1 (Patent) 1998.
30. Tobias Daßler TM, Christoph Winterhalter and August Böck Identification of a major facilitator protein from *Escherichia coli* involved in efflux of metabolites of the cysteine pathway. *Mol Microbiol.* 2000;36:1101–12.
31. Umenhoffer K. Reduced evolvability of *Escherichia coli* MDS42, an IS-less cellular chassis for molecular and synthetic biology applications. *Microb Cell Fact.* 2010. <https://doi.org/10.1186/1475-2859-9-38>.
32. Csorgo B, Feher T, Timar E, Blattner FR, Posfai G. Low-mutation-rate, reduced-genome *Escherichia coli*: an improved host for faithful maintenance of engineered genetic constructs. *Microb Cell Fact.* 2012;11:11.
33. Liu H, Wang Y, Hou Y, Li Z. Fitness of chassis cells and metabolic pathways for L-cysteine overproduction in *Escherichia coli*. *J Agric Food Chem.* 2020;68(50):14928–37.
34. Mamum AAMA. Identity and function of a large gene network underlying mutagenic repair of DNA breaks. *Sci Rep.* 2012;338:1344–8.
35. Loddeke M, Schneider B, Oguri T, Mehta I, Xuan Z, Reitzer L. Anaerobic cysteine degradation and potential metabolic coordination in *Salmonella enterica* and *Escherichia coli*. *J Bacteriol.* 2017. <https://doi.org/10.1128/JB.00117-17>.
36. Nonaka G, Takumi K. Cysteine degradation gene yhaM, encoding cysteine desulfidase, serves as a genetic engineering target to improve cysteine production in *Escherichia coli*. *AMB Express.* 2017;7(1):90.
37. Bertheau O. A new type of bacterial sulfatase reveals a novel maturation pathway in prokaryotes. *J Biol Chem.* 2006;281:22464–70.
38. Ploeg JRvd. Identification of sulfate starvation-regulated genes in *Escherichia coli*, a gene cluster involved in the utilization of taurine as a sulfur source. *J Bacteriol.* 1996. <https://doi.org/10.1128/jb.178.18.5438-5446.1996>.
39. van Der Ploeg JR, Iwanicka-Nowicka R, Bykowski T, Hryniewicz MM, Leisinger T. The *Escherichia coli* ssuEADCB gene cluster is required for the utilization of sulfur from aliphatic sulfonates and is regulated by the transcriptional activator Cbl. *J Biol Chem.* 1999;274(41):29358–65.
40. Sirko A. Sulfate and thiosulfate transport in *Escherichia coli* K-12: nucleotide sequence and expression of the CysTWAM gene cluster. *J Bacteriol.* 1990. <https://doi.org/10.1128/jb.172.6.3351-3357.1990>.
41. Kertesz MA. Proteins induced by sulfate limitation in *Escherichia coli*, *Pseudomonas putida*, or *Staphylococcus aureus*. *J Bacteriol.* 1993. <https://doi.org/10.1128/jb.175.4.1187-1190.1993>.
42. Leyh TS, Vogt TF, Suo Y. The DNA sequence of the sulfate activation locus from *Escherichia coli* K-12. *J Biol Chem.* 1992;267(15):10405–10.
43. Ostrowski J, Wu JY, Rueger DC, Miller BE, Siegel LM, Kredich NM. Characterization of the *cysJH* regions of *Salmonella typhimurium* and *Escherichia coli* B. *J Biol Chem.* 1989;264(26):15726–37.
44. Tanaka Y. Crystal structure of a YeeE-YedE family protein engaged in thiosulfate uptake. *Sci Adv.* 2020. <https://doi.org/10.1126/sciadv.aba7637>.
45. Haas M, Rak B. *Escherichia coli* insertion sequence IS150: transposition via circular and linear intermediates. *J Bacteriol.* 2002;184(21):5833–41.
46. Chen CS, Korobkova E, Chen H, Zhu J, Jian X, Tao SC, et al. A proteome chip approach reveals new DNA damage recognition activities in *Escherichia coli*. *Nat Methods.* 2008;5(1):69–74.
47. Kumar A, Beloglazova N, Bundalovic-Torma C, Phanse S, Deineko V, Gagarinova A, et al. Conditional epistatic interaction maps reveal global functional rewiring of genome integrity pathways in *Escherichia coli*. *Cell Rep.* 2016;14(3):648–61.
48. Posfai G, Plunkett G 3rd, Feher T, Frisch D, Keil GM, Umenhoffer K, et al. Emergent properties of reduced-genome *Escherichia coli*. *Science.* 2006;312(5776):1044–6.
49. Kumar PK. Strategies for improving plasmid stability. *Trends Biotechnol.* 1991;9:279–84.
50. Ikeda M. Amino acid production process. In: Robert Faurie JT, Bathe B, Debabov VG, Huebner S, Ikeda M, Kimura E, Marx A, Möckel B, Mueller U, Pfefferle W, editors. *Advances in Biochemical Engineering/Biotechnology.* Berlin: Springer; 2003.

51. Stanbury PF, Whitaker A, Hall SJ. Principles of fermentation technology. Amsterdam: Elsevier; 2013.
52. Park MK, Lee SH, Yang KS, Jung SC, Lee JH, Kim SC. Enhancing recombinant protein production with an *Escherichia coli* host strain lacking insertion sequences. *Appl Microbiol Biotechnol*. 2014;98(15):6701–13.
53. Zhong S, Dean AM. Rapid identification and mapping of insertion sequences in *Escherichia coli* genomes using vectorette PCR. *BMC Microbiol*. 2004;4:26.
54. Gaitonde MK. A spectrophotometric method for the direct determination of Cysteine in the presence of other naturally occurring amino acids. *Biochem J*. 1967;104:627–33.
55. Liao Y, Smyth GK, Shi W. featureCounts: an efficient general purpose program for assigning sequence reads to genomic features. *Bioinformatics*. 2014;30(7):923–30.
56. Robinson MD. A scaling normalization method for differential expression analysis of RNA-seq data. *Genome Biol*. 2010. <https://doi.org/10.1186/gb-2010-11-3-r25>.
57. Robinson MD, McCarthy DJ, Smyth GK. edgeR: a bioconductor package for differential expression analysis of digital gene expression data. *Bioinformatics*. 2010;26(1):139–40.

### Publisher's Note

Springer Nature remains neutral with regard to jurisdictional claims in published maps and institutional affiliations.

Ready to submit your research? Choose BMC and benefit from:

- fast, convenient online submission
- thorough peer review by experienced researchers in your field
- rapid publication on acceptance
- support for research data, including large and complex data types
- gold Open Access which fosters wider collaboration and increased citations
- maximum visibility for your research: over 100M website views per year

At BMC, research is always in progress.

Learn more [biomedcentral.com/submissions](https://biomedcentral.com/submissions)

